

Feedback Control Formulations for a Complex Flexible Structure
Utilizing Reaction Mass Actuators

1991

Ephraim Garcia†
Research Assistant Professor

Brett James Pokines and Robert Alan Carlin
Graduate Assistants

Department of Mechanical and Aerospace Engineering
State University of New York at Buffalo
Buffalo, New York 14260

Captain Steven Webb
Assistant Professor
Department of Engineering Mechanics
US Air Force Academy, Colorado 80840

DTIC
ELECTE
MAR 28 1991
S B D

Abstract

Active control has been performed on a structure possessing complex modal behavior. This structure had closely spaced modes, creating a "beat phenomena" in the structure's free vibration. The dynamic characteristics of the actuators are reported and a model for the interaction of actuator and structure is developed. Reaction mass actuators (RMAs) were analyzed with two control schemes. A local velocity feedback (LVF) controller was designed and implemented. A full state feedback controller was designed and evaluated on an experimentally verified analytical model of the flexible structure. Various linear quadratic regulator (LQR) control laws were considered and compared to the LVF controller. An investigation was performed using the LQR controller that investigated the effects of the stroke length with a full state feedback controller.

1. Introduction

Flexible space structures will require some form of control to minimize or eliminate undesirable vibrations. This has driven researchers to examine various schemes of active control to suppress a structure's vibration. Many analytical studies are based on a linear quadratic (LQ) optimal control scheme [1]. Fundamental to LQ controllers is the linear quadratic regulator (LQR); this controller is based on the assumption that all full states of the system model, the states of the structure and actuators, are available to each of the controllers [2]. Unfortunately, it is difficult to implement an LQR control scheme since it is almost always necessary to develop an observer to estimate the states in the system. Often the LQR controller is based on a reduced-order

model of the structure, which introduces uncertainties and perhaps instabilities in the higher-order modes [1]. These issues have driven many experimental studies to examine simpler control laws [1,3,4].

The purpose of this paper is to first develop one such simple controller, that is, its design and experimental implementation into a structure with complex modal behavior. Secondly, an LQR controller will be designed and compared to the LVF controller. The dynamic characteristics of the actuator and structure are reported.

2. Experimental System Description

An experimental (Figure 1) apparatus was employed to study the ability of RMAs (Figure 2) to control the vibrations of a structure with closely coupled modes. This test bed system is known as the MRT structure (mass reactive T structure). This structure was designed to have low order coupling - there were to be two dominant low-frequency structural modes, and the higher modes were to possess frequencies at least three times that of the first mode [5]. The structure weighs approximately 240 pounds and is very lightly damped. Each RMA reaction mass has a weight of only 4 pounds. Applying two actuators to this vibration suppression problem yields an actuator mass to structural mass ratio of approximately 3%.

The MRT structure was modeled using a 48-degree of freedom MSC/NASTRAN model. From this model, a reduced fourth order model was then selected such that the first two structural modes (the modes to be controlled) were as accurate as possible. This model reduction was based on an accurate reduction technique

† Also a Research Associate at the Frank J. Seiler Research Laboratory,
US Air Force Academy, Colorado.

reduction was based on an accurate reduction technique outlined by Hallauer and Barthelemy [6]. For the configuration shown in Figure 1, the structure's first resonant frequency corresponded to a torsional, or twisting, motion about the z-axis. The second frequency corresponded to a bending motion about the x-axis.

The analytical model was then validated by making a comparison to the experimental structure. To verify the analytical model, the structure's open loop resonant frequencies were determined and compared to the analytical modes (refer to Table 1). The modal damping in the baseline structure was identified using SDRC's Polyreference software and is reported in Table 2. Since, it is of interest to control the first two modes of vibration the model retains four modes because of potential spillover effects [7].

3. System Dynamics

The dynamics of the system will be broken into two parts. First, the dynamics of the RMA will be investigated, and the critical constants for modeling the dynamics of the RMA will be reported. Second, the overall system dynamics, that is, the dynamics of the interaction of the structure and actuator will be modeled.

Reaction Mass Actuator Dynamics

From the block diagram of Figure 3, the circuit gain representation of the damping and stiffness may be obtained. To find these gains, consider the transfer function of the PD controller,

$$\frac{x_{Ri}(s) - x_s(s)}{f_{CMD}(s)} = \frac{K_{amp} K_{coil}}{m_{Ri} s^2 + (C_0 + K_{damp})s + K_{stiff}} \quad (1)$$

where

$$K_{damp} = K_v K_{coil} K_{amp} K_{LVT}$$

$$K_{stiff} = K_{amp} K_{coil} K_p K_{probe}$$

The term, m_{Ri} , is the reaction mass of the RMA and C_0 is the internal damping of the actuator. The values of the coefficients in Eq. (1) are reported by Garcia [8].

Actuator/Structure Interaction

The dynamics of the combined actuator and structure can be represented with second order dynamics [9]. This model combines the dynamics of the baseline structure (the structure without actuators) with the dynamics of the reaction mass actuators.

$$M\ddot{x} + D\dot{x} + Kx = B_f f_g \quad (2)$$

where

$$M = \begin{bmatrix} m_{R1} & 0 & 0 & 0 & 0 & 0 \\ 0 & m_{R2} & 0 & 0 & 0 & 0 \\ 0 & 0 & & & & \\ 0 & 0 & & M_s & & \\ 0 & 0 & & & & \\ 0 & 0 & & & & \end{bmatrix}$$

$$D = \begin{bmatrix} c_{R1} & 0 & -c_{R1} & 0 & 0 & 0 \\ 0 & c_{R2} & 0 & 0 & 0 & -c_{R2} \\ -c_{R1} & 0 & & & & \\ 0 & 0 & & D_s + D_R & & \\ 0 & 0 & & & & \\ 0 & -c_{R2} & & & & \end{bmatrix}$$

$$K = \begin{bmatrix} k_{R1} & 0 & -k_{R1} & 0 & 0 & 0 \\ 0 & k_{R2} & 0 & 0 & 0 & -k_{R2} \\ -k_{R1} & 0 & & & & \\ 0 & 0 & & K_s + K_R & & \\ 0 & 0 & & & & \\ 0 & -k_{R2} & & & & \end{bmatrix}$$

$$B_f^T = \begin{bmatrix} 1 & 0 & -1 & 0 & 0 & 0 \\ 0 & 1 & 0 & 0 & 0 & -1 \end{bmatrix}$$

The coefficients c_{Ri} and k_{Ri} represent the individual damping and stiffness constants for each RMA, as determined in the previous section. The matrices K_R and D_R are defined as,

$$K_R = \begin{bmatrix} k_{R1} & 0 & 0 & 0 \\ 0 & 0 & 0 & 0 \\ 0 & 0 & 0 & 0 \\ 0 & 0 & 0 & k_{R2} \end{bmatrix} \quad (3)$$

$$D_R = \begin{bmatrix} c_{R1} & 0 & 0 & 0 \\ 0 & 0 & 0 & 0 \\ 0 & 0 & 0 & 0 \\ 0 & 0 & 0 & c_{R2} \end{bmatrix} \quad (4)$$

The structural damping matrix was reconstructed using a modal damping assumption where the matrix S_m represents the mass weighted normalized eigenfunctions of the model [10],

$$D_s = S_m \text{DIAG}[2\zeta_1\omega_1, \dots, 2\zeta_4\omega_4] S_m^T \quad (5)$$

The control vector, f_g , is of the form

$$f_g = [f_{g1} \ f_{g2}]^T \quad (6)$$

The force term, f_{gi} , is a function of the force/voltage constant of the RMA and the voltage command signal, f_{CMD} (see Figure 3).

4. Local Velocity Feedback Control

For this study, it was desired to implement, for each RMA, a simple active control strategy involving local

velocity feedback (LVF). This control strategy was employed in order to take advantage of its low authority controller characteristics; that is, the actuators apply control forces which are governed only by sensors physically collocated to the RMA assemblies. The inputs to Eq. (1) are set equal to,

$$f_{gi} = k_{gi} \dot{x}_i \quad (7)$$

where $i = 3$ or 6 . Here all sensors are carried on the RMA, while the control law is performed off-line on an analog computer; on-board controller circuits have been incorporated into some RMA designs [9].

To implement LVF control, both actuators were first passively tuned. Several procedures exist for calculating the optimum frequency and damping ratio to which to tune each RMA [11,12]. It was found that better performance could be achieved by *not* applying optimum tuning. Essentially, the LVF control strategy sacrifices damping in the actuator modes of the system to increase damping in the structural modes. This can be understood through an analysis of the poles of the system [13]. This analysis shows that as the gain of the LVF controller is increased the poles of the actuator dominated modes of the system approach the imaginary axis as the poles of the structure dominated poles move deeper into the left half plane. The principle of the optimally tuned passively damped absorber relies on the relative motion between the structure and the actuator to dissipate energy. This optimal tuning produces a lightly damped absorber that guarantees motion in the actuator, and hence, the dissipation of energy. This optimal absorber is generally too lightly damped to yield any significant performance in the LVF control scheme. This is because the poles of the actuator dominated modes of the system are too close to the imaginary axis and as the LVF controller gain is increased, the actuator destabilizes.

A comparison of the open loop and closed loop system time histories is given in Figure 4, for the response of the structure at the actuator locations. The open loop settling time exceeded 500 seconds, and for the closed loop system the settling time dropped to 1.5 seconds. The analytical response for the closed loop system is shown in Figure 5.

5. Linear Quadratic Regulator Control

The second part of our analysis was to implement an LQR control law on the MRT structural model and analyze the effects of various weighting matrices. In particular, it was of interest to study the performance of the system when varying relative penalties between the penalty on the absolute motion of the structure versus the relative motion (or stroke length) of the actuator. The system in Eq. (2) can be cast into the following state space representation for the structure [10]

$$\dot{\mathbf{x}} = \mathbf{A}\mathbf{x} + \mathbf{B}\mathbf{u} \quad (8)$$

with output measurements defined by

$$\mathbf{y} = \mathbf{C}\mathbf{x} \quad (9)$$

The standard linear quadratic regulator has a performance functional of the form

$$J = \int_0^{\infty} (\mathbf{x}^T \mathbf{Q} \mathbf{x} + \mathbf{u}^T \mathbf{R} \mathbf{u}) dt \quad (10)$$

where \mathbf{Q} and \mathbf{R} are weighting matrices. The value of the feedback gain matrix \mathbf{K}_f is found such that the cost functional of Eq. (10) is minimized. State feedback control is implemented by specifying the relation

$$\mathbf{u} = -\mathbf{K}_f \mathbf{x} = \mathbf{R}^{-1} \mathbf{B}^T \mathbf{S} \mathbf{x} \quad (11)$$

and the optimum value of the performance index, J , given an initial condition, $\mathbf{x}(0)$, is

$$J = \mathbf{x}(0)^T \mathbf{S} \mathbf{x}(0) \quad (12)$$

where \mathbf{S} is found by solving an algebraic matrix Riccati equation [14].

Various methods exist for choosing suitable \mathbf{Q} and \mathbf{R} matrices. From our experimental observations the importance of the actuator stroke length in the performance of the system became clear, hence, the \mathbf{Q} matrix was defined as

$$\mathbf{Q} = \begin{bmatrix} \mathbf{Q}_s & \mathbf{0} \\ \mathbf{0} & \mathbf{Q}_s \end{bmatrix}$$

where the submatrix is

$$\mathbf{Q}_s = \begin{bmatrix} w_{act} & 0 & -w_{act} & 0 & 0 & 0 \\ 0 & w_{act} & 0 & 0 & 0 & -w_{act} \\ -w_{act} & 0 & w_{struc} & 0 & 0 & 0 \\ 0 & 0 & 0 & w_{struc} & 0 & 0 \\ 0 & 0 & 0 & 0 & w_{struc} & 0 \\ 0 & -w_{act} & 0 & 0 & 0 & w_{struc} \end{bmatrix}$$

The weighting coefficients w_{struc} and w_{act} determined the penalty on the absolute displacement of the structure and the relative displacement of the reaction mass, respectively. This relative displacement can be thought of as the stroke length of the actuator. The penalty on the controller was defined as

$$\mathbf{R} = 1.0e-03 \mathbf{I}$$

where w_{struc} was set to 1000. Here we will examine the results of setting w_{act} to [1, 10, 100, 1000] to illustrate the effects of stroke length on performance. The results of this study are presented in Table 3. Also

reported in this table are the maximum normalized stroke length of the actuator for each controller. This term is considered here to be the absolute maximum of the actuator's stroke normalized to the absolute maximum of the deflection of the structure. This normalized stroke length determines how many times larger the stroke length must be relative to the absolute structural displacement.

A vibration suppression index was formulated from the time response histories for each feedback control produced from the varying penalty functions. This index quantifies the performance of each case, i.e., the lower the number, the greater the vibration attenuation. The values of this index were calculated with the relation:

$$VSI = \frac{1}{t_f} \int_0^{t_f} w_{\text{struc}} \|x_{\text{struc}}\| dt$$

where x_{struc} is the response matrix of the structure. Clearly, Table 3 shows that as the penalty is reduced on the stroke of the actuator the performance of the system greatly increases. As the performance of the system increases the stroke length requirements of the actuator also increase. Physically, this makes sense, since it is the reaction force applied to the structure of the accelerating RMA masses which produce the control forces for vibration attenuation. Figures 6 are the time histories for the displacement of the structure at RMAs 1 for the given initial condition.

Interestingly, the normalized maximum stroke length required for the LVF controlled response was 11.013. This value is consistent with those of the LQR controllers of Table 3. From the time histories of the LQR and LVF controller we can say that the performance of the LVF controller is better than the LQR controller when $w_{\text{act}}=100$, and worse than the LQR when $w_{\text{act}}=10$. The normalized maximum stroke length for the LVF controller was between the two values of the LQR controllers for $w_{\text{act}}=10$ and 100. This indicated that for either this simple low authority controller or the full state feedback regulator, the underlying factor determining performance is the stroke length of the actuator.

6. Closing Remarks

A simple feedback control law based on a local velocity signal has been designed and implemented into a complex flexible structure. It was shown that although the actuator to structure mass ratio for the system was only 3% the closed loop settling time was reduced to 1.5 seconds where the open loop system settling time for the system was approximately 500 seconds. Experimentally it was observed that the LVF feedback controller drove the RMA mass to react, or accelerate, against the structural motion. Logically, the faster the actuator mass accelerates, more stroke length is required to permit the resulting motion. Hence, the actuator

stroke length governed the performance of the RMA actuated system. This was also studied by applying an LQR controller which also showed a strong dependence on the actuator stroke length. Furthermore, the LVF control law performed nearly the same as the LQR controller when both controllers used the same degree of actuator stroke length.

Acknowledgement

This work was supported through the AFOSR Summer Faculty Research Program and the Graduate Student Research Program administered by the Universal Energy Systems Corporation, grant no. F49620-88-C-0053. This work was performed at the Frank J. Seiler Research Laboratory located at the US Air Force Academy, Colorado. The authors gratefully acknowledge the assistance of Mr. Jim Smith and Captain Jeff Turcotte.

References

- [1] Martinovic, Z.N., Schamel, G.C. II, Haftka, R.T., and Hallauer, W.L., Jr., "Analytical Investigation of the Output Feedback vs Linear Quadratic Regulator," *AIAA Journal of Guidance, Control and Dynamics*, vol. 13, no. 1, Jan.-Feb. 1990, pp. 160-167.
- [2] Meirovitch, L., *Dynamics and Control of Structures*, John Wiley & Sons, New York, 1990.
- [3] Skidmore, G.R., and Hallauer, W.L., Jr., "Experimental-Theoretical Study of Active Damping with Dual Sensors and Actuators," *Proceedings of the AIAA/ASME/AHS 27th Structures, Structural Dynamics and Materials Conference*, pt 2, AIAA, New York, 1986, pp. 613-620.
- [4] Zimmerman, D.C. and Inman, D.J., "On the Nature of the Interaction Between Structures and Proof-Mass Actuators," *AIAA Journal of Guidance, Control, and Dynamics*, Vol. 13, No. 1, Jan.-Feb. 1990, pp. 82 - 88.
- [5] Webb, S.G. and Turcotte, J.S., "Analysis of a Passively Tuned Actuator on a Low-Order Structure," *1990 AIAA Guidance, Navigation, and Control Conference*, AIAA Paper 90-3500, August, 1990.
- [6] Hallauer, W.L., Jr., and Barthelemy, J.-F.M., "Active Damping of Modal Vibrations by Force Apportioning," *21st AIAA Structures, Structural Dynamics, and Materials Conference*, 1980, Paper 80-0806 in AIAA CP804, Part 2, pp. 863-873.
- [7] Balas, M.J., "Observer Stabilization of Singularly Perturbed Systems," *AIAA Journal of Guidance, Control, and Dynamics*, Vol. 1, No. 1, Jan.-Feb. 1978, pp. 93-95.
- [8] Garcia, E., Pokines, B.J., Carlin, R.A., "Control of a Complex Flexible Structure Utilizing Space-Realizable Linear Reaction Mass Actuators," Final Report, Universal Energy Systems, Inc., AFOSR, Contract no. F49620-88-C-0053, September 7, 1990.
- [9] Zimmerman, D.C., Horner, G.C., and Inman, D.J., "Microprocessor Controlled Force Actuator," *AIAA Journal of Guidance, Control and Dynamics*, Vol. 11, No. 3, May-June, 1988, pp.230-236.

- [10] Inman, D.J., *Vibration with Control, Measurement, and Stability*, Prentice-Hall, Englewood Cliffs, New Jersey, 1989
- [11] Duke, J.P., Webb, S.G. and Vu, H., "Optimal Passive Control of Multi-Degree of Freedom Systems Using a Vibration Absorber," 1990 AIAA Guidance, Navigation, and Control Conference, AIAA Paper 90-3499, August, 1990.
- [12] Juang, J.-N., "Optimal Design of a Passive Vibration Absorber for a Truss Beam," *AIAA Journal of Guidance, Control, and Dynamics*, Vol. 7, No. 6, Nov.-Dec. 1984, pp. 733-739.
- [13] Garcia, E., Webb, S., Duke, J., "Passive and Active Control of a Complex Flexible Structure Using Reaction Mass Actuators," *Eighth VPI&SU Symposium on Dynamics and Control of Large Structures*, Blacksburg, Virginia, May 6-8, 1991.
- [14] Kwakernaak, H. and Sivan, R., *Linear Optimal Control Systems*, Wiley, New York, 1972.

Analytical (Hz)	Experimental (Hz)	Percent Error (%)
4.6417	4.618	0.5
5.1904	5.113	1.5
109.4542	89.669	22.1
163.1361	129.109	26.3

Table 1. Analytical and Experimental Structural Resonant Frequencies.

Mode	Damping Ratio (% critical)	Modal Confidence Factor
1	.079	0.999
2	.267	0.994
3	.169	0.998
4	.314	0.998

Table 2. Modal Analysis - Polyreference identified damping factors.

Actuator Weighting wact	Normalized Max. Stroke Length	Cost, J	Vibration Suppression Index
1.0	29.342	2,322	.0356
10	17.381	4,481	.0665
100	6.4272	12,253	.1967
1000	0.7886	14,378	1.5000

Table 3. Performance cost and stroke length requirements for various degrees of penalty on actuator stroke.

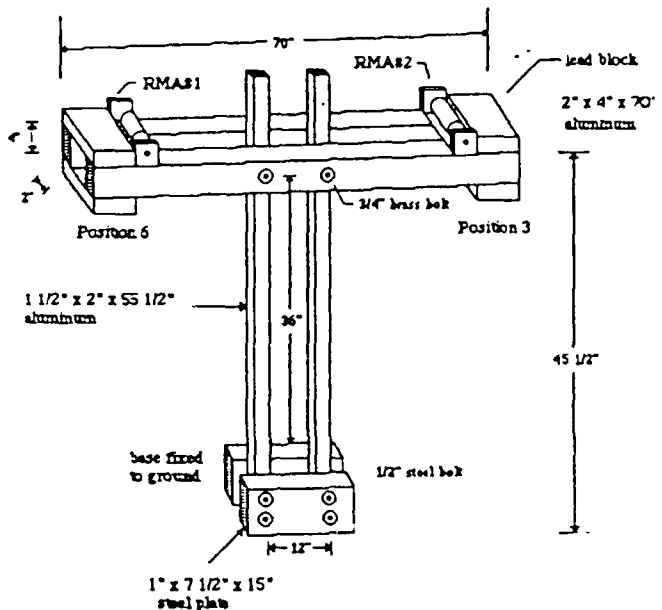


Figure 1. Schematic representation of the MRT structure.

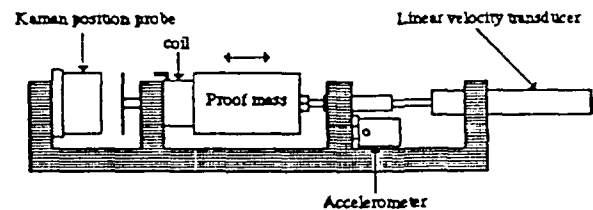


Figure 2. Schematic of the RMA assembly - side view.

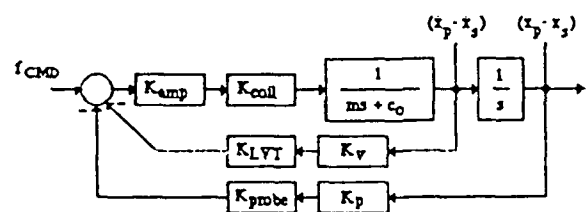


Figure 3. Block diagram of the Reaction Mass Actuator Control Circuit.

OF	
DTIC TAB	<input checked="" type="checkbox"/>
Unannounced	<input type="checkbox"/>
Justification	<input type="checkbox"/>
By <i>per Form 50</i>	
Distribution/	
Availability Codes	
Dist	Avail and/or Special
<i>A-1</i>	

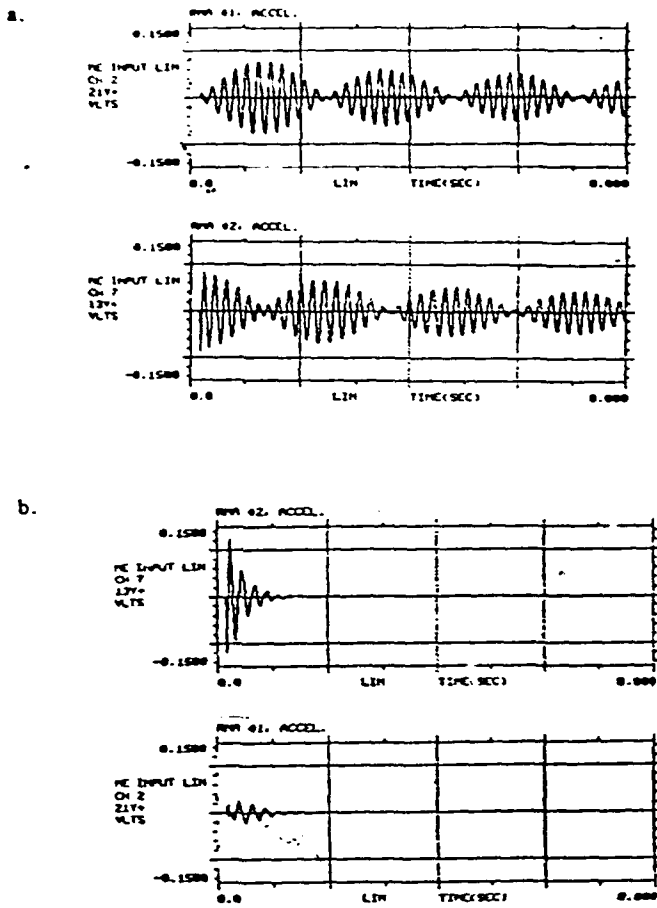


Figure 4. Open (a) and closed loop LVF control (b) time histories for RMAs 1 and 2.

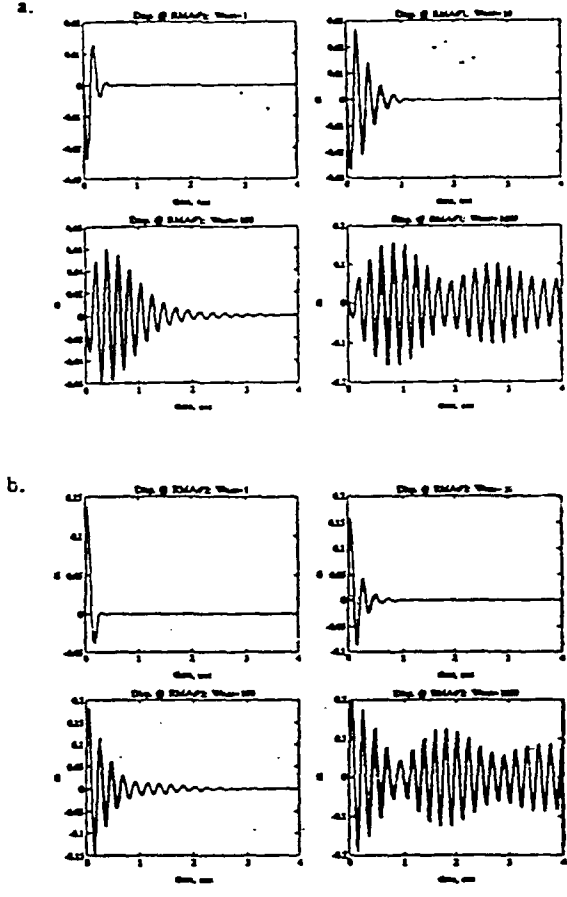


Figure 6. Free decay responses at RMAs 1(a) and 2 (b) for various LQR feedback controllers.

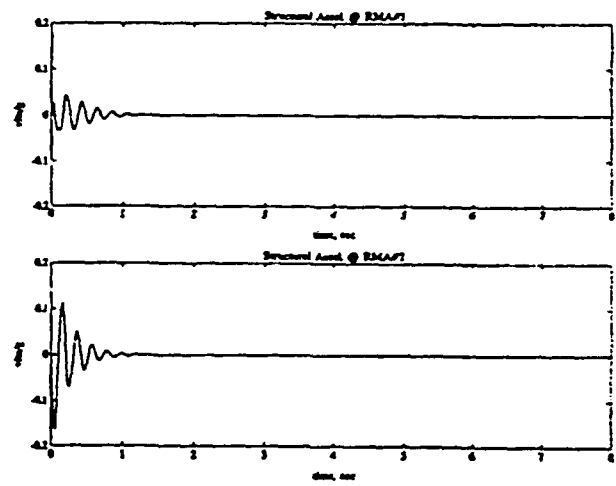


Figure 5. Analytical Response of the closed loop LVF control system.